12th International Symposium on Turbulence and Shear Flow Phenomena (TSFP12)
Osaka, Japan (Online), July 19-22, 2022

INFLUENCE OF A CYLINDER INSTALLED UPSTREAM ON THE FLOW FIELD OF A TURBULENT JET

Srikar Yadala*, Girish K. Jankee, Eirik Æsøy, James R. Dawson & Nicholas A. Worth
Department of Energy and Process Engineering
Norwegian University of Science and Technology
Trondheim N-7491, Norway
*srikar.y.venkata@ntnu.no

ABSTRACT

The influence of a cylinder installed upstream of a round jet's exit plane on the dynamics of this flow field is investigated. Acoustic excitation is used to excite the flow at a particular frequency and phase-locked, high-resolution particle image velocimetry is employed to obtain velocity data. The cylinders have a marginal effect on the mean flow field. However, the circulation within the vortical flow structures reduces, which ultimately leads to a decrease in the strength of the fluctuating quantities. There is also evidence of the cylinders' potential in increasing the three-dimensionality of the jet flow. The results demonstrate that the vortex shedding in the cylinders' wake modifies the boundary condition at the jet's exit and thus, affects the shear layer and the jet flow field as a whole.

INTRODUCTION

Round jets that discharge into surrounding ambient fluid have been studied extensively in the past decades. The interaction of the jet with the ambient fluid gives rise to a free-shear layer in the near field which is influenced by axisymmetric Kelvin-Helmholtz and helical instabilities (Crow & Champagne, 1971; Ho & Huerre, 1984). The Kelvin-Helmholtz (primary) instability waves yield regions of concentrated vorticity that encircle the jet's potential core and propagate downstream. The secondary (helical) instabilities induce streamwise vorticity within the primary vortical structures and contribute to their eventual breakdown. There has been significant interest in manipulating the Kelvin-Helmholtz mechanism through the modification of the jet's inlet boundary conditions (see for example Crow & Champagne, 1971; Ho & Huerre, 1984; Aydemir *et al.*, 2012). The aim of such research can be to better understand the fundamental response of the jet to certain input conditions or to affect other aspects further downstream such as turbulent statistics, mixing rate, jet noise and heat transfer among others.

The majority of research efforts have focused on measuring the jet's response to axisymmetric disturbances (for example, Crow & Champagne, 1971; Aydemir *et al.*, 2012). Only a few studies have attempted to understand the impact of asymmetric forcing, which was summarised by Reynolds *et al.* (2003). Asymmetric forcing can be achieved (for example) through transverse acoustic disturbances as demonstrated recently by Worth *et al.* (2020) and Æsøy *et al.* (2021*b*). The predominant effect in such cases is an inclination change in successive vortical structures and for some conditions, bifurcation of the jet into separated momentum streams each carrying a portion of the total momentum. A second method is to use geometrical features as a form of passive flow control. These features can be a modified shape of the jet nozzle's trailing edge (Longmire *et al.*, 1992; Longmire & Duong, 1996) or the use vortex generators (Reeder & Samimy, 1996). In these cases, the amplification of secondary instabilities and corrugation of the primary vortical structures have been demonstrated.

The objective of the current research is to investigate and understand the influence of a cylinder installed upstream of the jet exit on the evolution of vortical structures and thereby the near-field dynamics. In practical situations, jet flows are often not well conditioned due to design constraints which can introduce disturbances that modify the flow in unexpected ways. One such example is the study of acoustically forced flames by Æsøy *et al.* (2021*a*) which showed that vortex shedding from upstream geometries can couple with acoustic oscillations to modify the flame response. These findings were in fact the motivation behind the current research efforts. As such, the use of a cylinder is to replicate such scenarios in practical applications, albeit in a simplified manner.

EXPERIMENTAL SETUP AND MEASUREMENT SYSTEMS

The axisymmetric jet used by Aydemir *et al.* (2012) (also by Worth *et al.*, 2020; Æsøy *et al.*, 2021*b*) was modified and employed in the current investigation. A schematic of the experimental set-up is shown in figure 1. The apparatus consists of a 200 mm long cylindrical plenum chamber with an inner diameter of 100 mm followed by a 350 mm long tube with an inner diameter of 35 mm. The apparatus is completed by a converging nozzle with a knife-edged exit to achieve a top-hat exit velocity profile. The convergence ratio of the nozzle is $12.25:1$ along the streamwise direction and it has an exit diameter of $D = 10$ mm (used henceforth to non-dimensionalize the spatial coordinates). The rate of air flow was regulated with a mass flow controller and fed into the facility below the plenum. As such, the bulk velocity of the jet was maintained at $U_b = 11\ (\pm 0.5)$ m s^{-1} for all tested cases and the Reynolds number based on the jet's exit diameter is $Re_D = 7483$. Axisymmetric acoustic excitation was employed to ensure vortex-structure formation at select frequencies. To this effect, harmonic velocity oscillations at the nozzle's exit were generated by two diametrically opposed loudspeakers installed on the plenum chamber. A *TTi 40 MHz* waveform generator provided monochromatic sinusoidal input signals at selected frequencies (f_e) to drive the loudspeakers. The amplitude of these

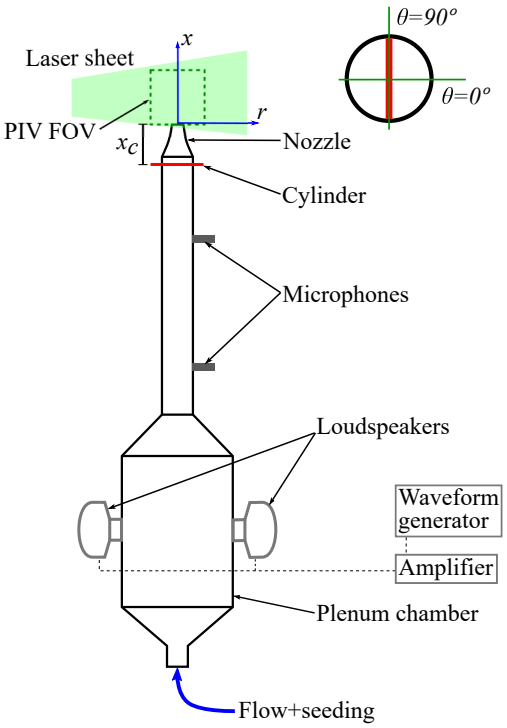

Figure 1: Schematic of the experimental set-up (not to scale). Inset at the top-right corner shows the two PIV planes captured.

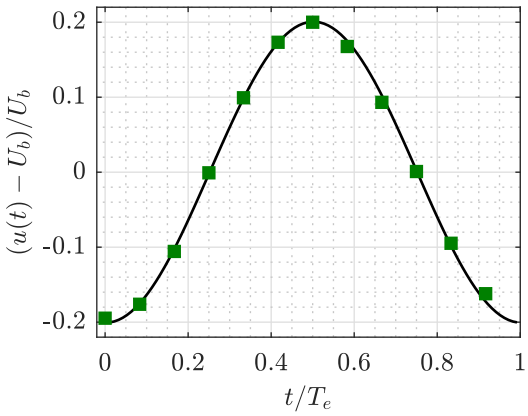

Figure 2: Acoustic fluctuation at the jet's exit plane (black curve) and PIV velocity measurement at $x/D = 0.2$ (green '**x**' in figure 3a) at different phases along the acoustic cycle (green markers).

Table 1: List of experimental conditions.

d_C (mm)	x_C (mm)	x_C/d_C
No cylinder	-	∞
2	70	35
6	104	17.3
6	70	11.7
10	87	8.7

acoustic velocity fluctuations ($A_e = u'(f_e)/U_b$) at the nozzle's exit was fixed using the multiple microphone method (Seybert & Ross, 1977) for which, pressure measurements at two streamwise stations along the 350 mm long pipe were obtained through *Brüel & Kjær free-field* $1/4''$ condenser microphones. The coordinate system is defined as follows: x and r represent the streamwise and radial directions respectively, with the origin being at the centre of the nozzle's exit. The corresponding velocity components are u and v respectively. For the cases with a cylinder installed upstream, θ represents the azimuthal angle, with $\theta = 0^\circ$ being perpendicular to the cylinder's length (see inset in figure 1).

Quantitative velocity measurements of the ensuing jet flow were obtained through a low-speed planar particle image velocimetry (PIV) system. The flow was seeded with olive oil droplets that were produced using a Laskin nozzle and introduced into the air flow upstream of the plenum. Illumination of these oil droplets was achieved with a *Litron Nano L* 200 mJ dual-pulse Nd:YAG laser, whose beam was shaped into a ≈ 1 mm thick light sheet. Imaging of the field-of-view (FOV) was carried out using a *LaVision Imager LX* 16 MP camera featuring a 4904×3280 px^2 sensor. The camera was equipped with a *Nikon-Nikkor* 200 *mm micro* lens operated at $f_\# = 8$ and was positioned normal to the imaging plane. The inspected planes were along the $x-r$ directions just above the nozzle exit (dashed (green) rectangle in figure 1) and up to $x/D \approx 5$ in order to capture the developing shear layer. Synchronisation of the laser pulses and camera timing was achieved using a *LaVision PTU* and the acquisition was at a sampling frequency of 1 Hz, in double-frame mode ($\Delta t = 10$ μs). Additionally, the PIV system was synchronised with the acoustic driving signal, thereby achieving a phase-locked measurement at 12 equidistant phases along the driving signal for all test cases. For each phase, 200 image pairs were captured. Image acquisition, pre-processing and vector computations were performed using *LaVision DaVis 10* software suite. Cross-correlation for vector field computation was carried out with a final interrogation window of 24×24 px^2 with a relative overlap of 50%, which resulted in a spatial resolution of 0.13 mm between vectors in both x and r directions.

The PIV system was first employed to acquire quantitative velocity data of the jet flow field with no cylinder installed. The time-average vector field of the streamwise velocity $\overline{u}$ is presented in figure 3a. The velocity of the jet just downstream of the exit at $x/D = 0.2$, $r/D = 0$ (green '**x**' in 3a) is $U_b = 11.03$ m s^{-1} (henceforth used to normalise different quantities as necessary), which agrees well with the bulk velocity set through the mass flow controller. The jet was conditioned through an acoustic excitation at a frequency of $f_e = 160$ Hz, with an amplitude $A_e = 0.2$ at the nozzle's exit for all test cases. The corresponding Strouhal number based on the jet's exit diameter and bulk velocity is $St_D = 0.15$. One time period (T_e) of the imparted acoustic fluctuation, computed using the multiple microphone method, is presented in figure 2. The velocity fluctuation measured at $x/D = 0.2$ at the different phases is also shown in the figure (solid green squares) and is seen to agree well with the imparted acoustic fluctuation. It is worth noting that this no cylinder case serves as the reference against which the influence of the cylinders will be compared. Three cylinders with different diameters d_C were installed at various upstream locations in order to ascertain the effect of such geometrical features on the jet's dynamics. The different test cases will henceforth be referred to by the ratio x_C/d_C, where x_C is the distance of the particular cylinder with respect to the jet's exit as illustrated in figure 1. The differ-

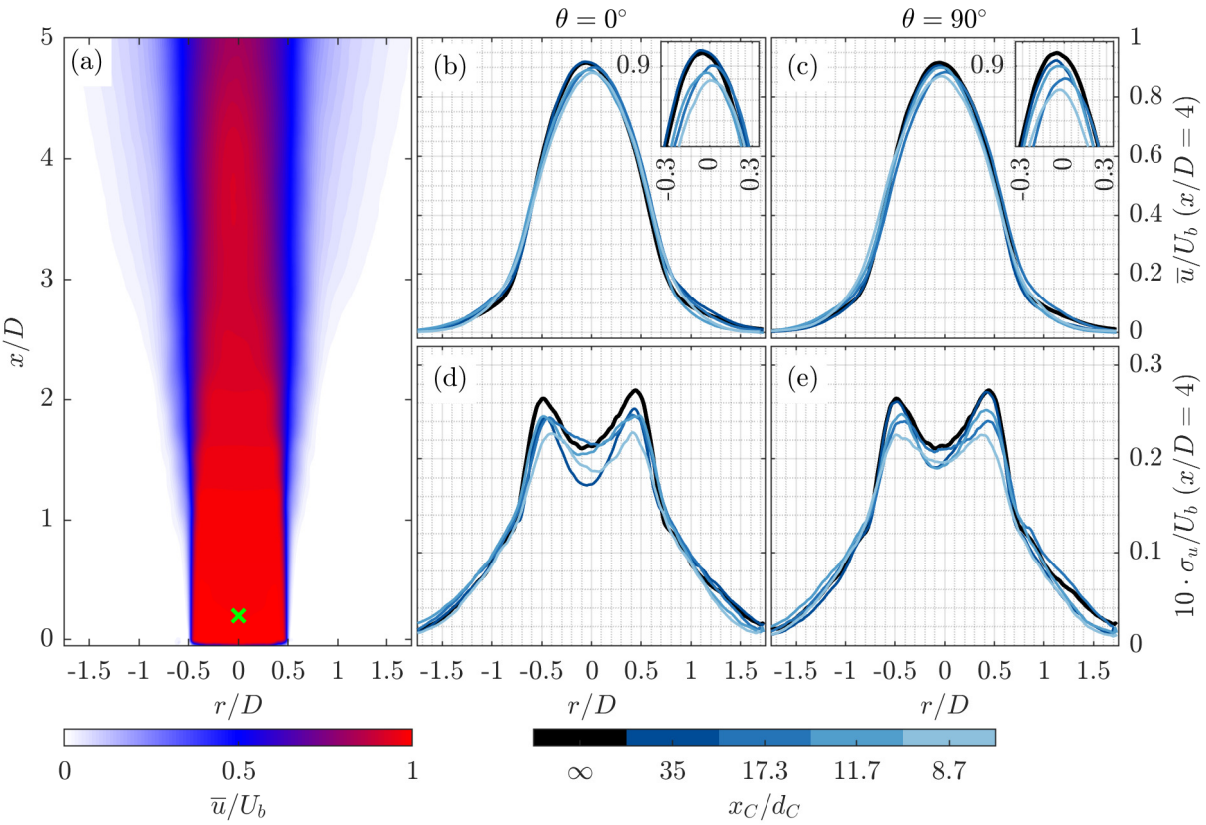

Figure 3: Statistical quantities. (a) Normalised $\overline{u}$-velocity contour for the no cylinder (reference) case; (b) & (c) Normalised $\overline{u}$-velocity profiles at $x/D = 4$ with insets showing a zoomed-in view; (d) & (e) Normalised σ_u profiles at $x/D = 4$.

ent test cases are listed in table 1. Also, for the cases with cylinders installed, PIV measurements were acquired at two different planes along the angular direction θ. The first plane was perpendicular to the cylinder's length while the second was parallel to it. These planes are referred to by the angles $\theta = 0°$ and $\theta = 90°$ respectively, in the rest of the document and are shown in the inset in figure 1.

RESULTS & DISCUSSION

Statistical quantities computed from the PIV acquisition are presented in figure 3. The normalised $\overline{u}$-velocity profile along the radial direction at $x/D = 4$ for the different test cases, at the two measured PIV planes, is presented in figures 3b and c respectively. Minor differences are observed at the edge of the jet, but this can be a result of the variable seeding density in this region and thus, can be discounted. Barring this, the streamwise velocity at the jet core is marginally lower when the cylinders are installed compared to the reference case, which is an artefact of the cylinder's wake. The reduction in velocity seems to scale with x_C/d_C (see insets in figures 3b & c). The change is negligible for the $x_C/d_C = 35$ test case and the maximum reduction is observed to be $\approx 5\%$ of the reference case for $x_C/d_C = 8.7$. While the contracting nozzle seems to aid in recovering the velocity deficit in the cylinder's wake and regularise the flow at the jet's exit to a great extent, the cylinders do leave a footprint on the mean flow field, albeit very small. In the absence of such a contracting section, one can expect this effect to be significantly amplified, depending on the upstream location of the cylinder.

While the mean velocity is affected marginally, the cylinders do impact the fluctuating quantities significantly as evidenced by the profiles of the standard deviation of the streamwise velocity (σ_u) at $x/D = 4$, shown in figures 3d and e. A general reduction in the strength of the fluctuations compared to the reference case is observed for all cases with an upstream cylinder. No clear trend is recognised in the jet core barring the general reduction. In the shear layer region on the other hand (around $r/D = \pm 0.5$), the fluctuations seems to reduce with x_C/d_C as observed with the mean velocity. The maximum reduction at this streamwise station again corresponds to the $x_C/d_C = 8.7$ case, with the change in the standard-deviation profile's maxima being a compelling $\approx 17\%$ compared to the reference case. Finally, except the $x_C/d_C = 35$ test case, the σ_u profiles at the two measured planes agree well with one another for the different cases. The reason for this exception with the $x_C/d_C = 35$ case cannot be ascertained with the available data and will be investigated upon in the future.

The brief discussion until now clearly indicates that the cylinders have an impact on the jet flow field, especially on the fluctuating quantities. These effects are investigated further through the phase-averaged velocity fields. The vorticity (ω) at the different phases were computed from the measured average velocity fields using a second-order central differences method and were normalised by multiplying with the ratio D/U_b. Such a normalised vorticity field from the different test cases at $t/T_e = 0.75$ along the acoustic cycle is presented in figure 4. Additionally, the swirl strength λ_{ci} (Adrian *et al.*, 2000), also normalised with D/U_b, is employed to detect vortical flow structures in the shear layer region. The results of these computations are superimposed on the presented vorticity fields as contour lines.

The initial development of the shear layer does not show a significant difference in all the tested cases. It is observed to

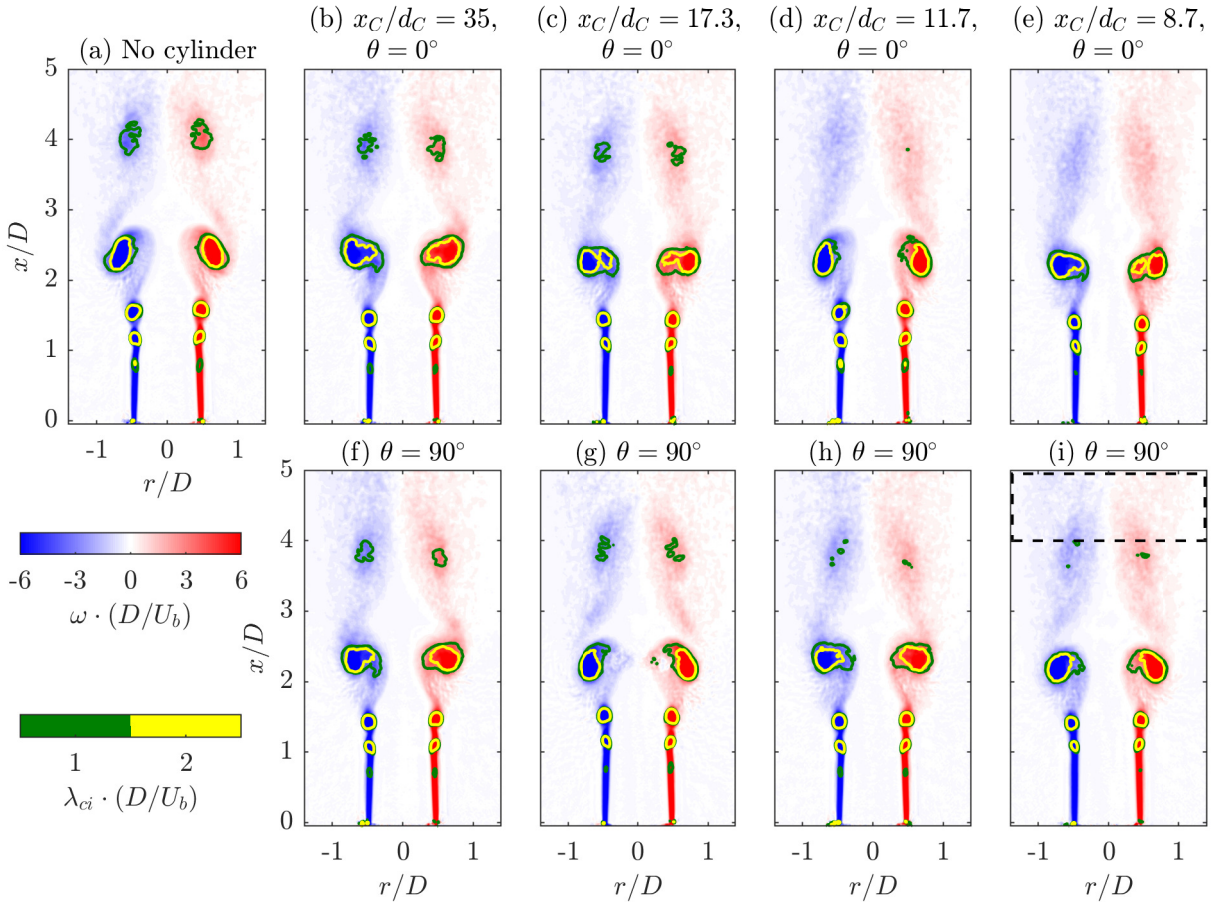

Figure 4: Phase-averaged vorticity distribution at $t/T_e = 0.75$ along the acoustic velocity fluctuation cycle at the jet's exit. Contour lines represent vortical flow structures detected through swirl-strength criterion.

roll-up into vortical flow structures around $x/D = 2.4$. These structures are a direct consequence of the acoustic excitation being applied. Furthermore, these vortical structures are at about the same streamwise station as in the reference case in both the $\theta = 0°$ and $\theta = 90°$ planes when a cylinder is installed upstream. This observation implies that the timing of the shear-layer roll up (and thereby the jet) is purely dictated by the acoustic mode and the installed cylinder has no influence on either the timing or the symmetry of the jet.

In the no cylinder case (figure 4a), a second vortical structure is observed around $x/D = 4$ which is the remnant of the smaller structure at $x/D \approx 15$ in the current snapshot, albeit from the previous acoustic cycle. The exisstence of this second vortical structure is unsurprising, given the low Strouhal number of the current acoustic excitation. It is well know that the jet's preferred mode is in the range of $0.24 \leq St_D \leq 0.64$ (Crow & Champagne, 1971). In the current set-up, significant jet response was observed in the range $0.3 \leq St_D \leq 0.5$ with a peak at $St_D = 0.33$ (see Æsøy *et al.*, 2021*b*). In comparison, the applied acoustic excitation at a Strouhal of $St_D = 0.15$ is slightly less than half the peak value and as such, will be the predominant mode only further downstream. This structure is also observed in the $x_C/d_C = 35$ and 17.3 cases at about the same streamwise location. However, its size and strength seems to diminish with x_C/d_C. In fact, in the last two cases ($x_C/d_C = 11.7$ and 8.7), the swirl-strength criterion does not even recognise the presence of a vortical structure. This trend of reducing vorticity magnitude around $x/D = 4$ with the x_C/d_C ratio corroborates well with the reduction in the standard deviation maxima discussed previously.

The circulation Γ will now be used as a metric to quantify this reduction in vortical-structure strength better. To this effect, the circulation in the region enclosed by the dashed (black) rectangle in figure 4i is computed at each phase along the acoustic cycle for every test case, according to equation 1.

$$\Gamma(t) = \int_x \int_r |\omega(x,r,t)| \cdot dr dx \tag{1}$$

The cumulative sum of $\Gamma(t)$ from each phase is then calculated and used as a measure of the total circulation Γ_{tot} in the considered interrogation domain. The circulation within the vortical flow structures (Γ_{vr}) present in the chosen domain is also pertinent. This was achieved by masking the vorticity magnitude field with a threshold iso-vorticity contour that defines the vortical structures' boundary as done in previous research efforts (Gharib *et al.*, 1998; Aydemir *et al.*, 2012). Through a sensitivity analysis, the appropriate threshold was found to be $\omega \cdot D/U_b > 1$ which corresponds to about 20% of the peak vorticity within the selected interrogation domain. It is worth noting that this threshold value is the same as that reported by Aydemir *et al.* (2012) in their work. The computed circulation (both Γ_{tot} and Γ_{vr}) is normalised by dividing with $(U_b \cdot D)$.

The evolution of circulation along the acoustic cycle for the different cases is presented in figures 5a and b. In all cases and in both PIV planes, the total circulation grows steadily until $t/T_e = 0.42$ beyond which, the rate of growth reduces a

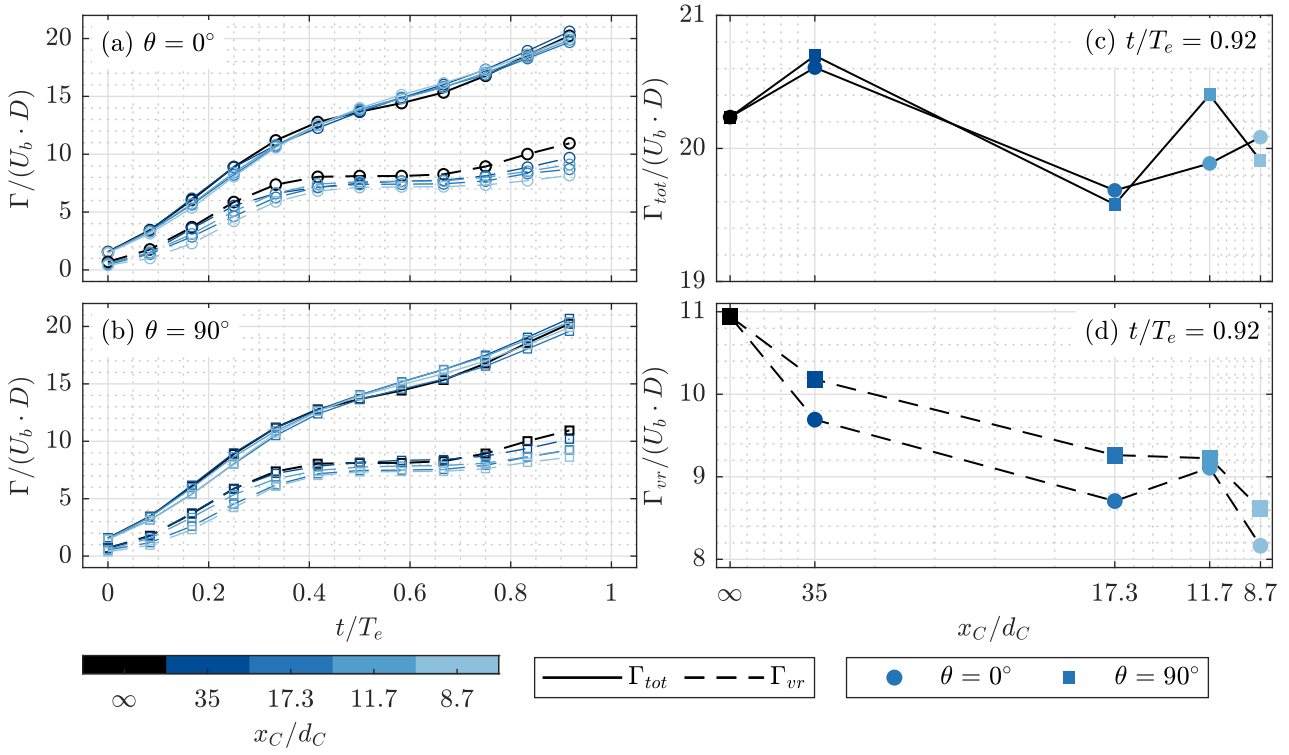

Figure 5: Normalised circulation (Γ_{tot} and Γ_{vr}) along the acoustic cycle for the different cases in the region enclosed by the dashed (black) rectangle in figure 4i. (a) $\theta = 0°$ plane; (b) $\theta = 90°$ plane; (c) and (d) Γ_{tot} and Γ_{vr} respectively, at $t/T_e = 0.92$.

little. The total circulation at the last phase along the acoustic cycle ($t/T_e = 0.92$) is plotted as a function of x_C/d_C in figure 5c to discern the impact of the cylinders. This particular phase is chosen with the assumption that these values of circulation will encompass all the flow dynamics within one acoustic cycle. While a specific scaling with x_C/d_C is not recognisable, it is clear that the cylinders do influence the total circulation.

Akin to the total circulation, the circulation based on the vorticity within vortical structures too, shows a gradual increase until $t/T_e = 0.42$. From here on and until $t/T_e = 0.67$, this component of circulation remains almost constant for all test cases. Beyond this, the circulation is seen to increase once again but at a lower rate. This feature is especially apparent in the reference case and is attributed to the weaker vortical structure that was seen in the phase-averaged vorticity fields close to $x/D = 4$ (see figure 4a). The cylinders installed upstream are seen to have a destructive effect on the vortical structures within the shear layer. This aspect is clearly noticeable in figure 5d where the circulation of the vortical structures at $t/T_e = 0.92$ as a function of x_C/d_C is plotted. The magnitude of Γ_{vr} is observed to diminish with this ratio, with the $x_C/d_C = 8.7$ test case demonstrating a reduction of about 25% with respect to the reference case.

A reduction in Γ_{tot} with respect to x_C/d_C, synonymous with Γ_{vr}, is expected but not observed. This discrepancy in the current results can be attributed to two aspects. Firstly, the computed vorticity fields were not treated with any spatial filters prior to the Γ_{tot} computation and as such, any background noise can impact the computed quantities. It is worth noting that the threshold applied to compute Γ_{vr} acts as a filter of some sort, making the distinctions between the different cases identifiable and trustworthy. Secondly, the observed discrepancy could be an attribute of the flow field, whereby the cylinders produce dynamics that are not synchronised with the acoustic cycle. These will therefore not be captured by the phase-locked measurement, but manifest as background vorticity in the different cases. These aspects will be investigated further in future works. Nonetheless, the curtailment of the vortical structure circulation is consistent with the decrease in the strength of fluctuations within the current jet flow field.

A decrease in the value of x_C/d_C essentially means the dynamics in the cylinder's wake that is perceived at the jet's exit plane is stronger. Thus, the fact that the decrease in different flow quantities is proportional to the ratio x_C/d_C implies that the vortex shedding in the cylinder's wake is responsible for any modulations of the fluctuations in the jet flow field. The vortices shed from the cylinders were not observed in any of the acquired cases. This can be attributed to the contracting nozzle which might be suppressing the vortical structure while retaining the induced fluctuations. Thus, a direct interaction of the shed vortices and the shear layer is discounted here. It is more probable, that the fluctuations within the cylinder's wake seeps into and modifies the incoming boundary layer, thereby affecting the shear-layer dynamics.

Finally, an interesting feature is brought to light when the Γ_{vr} computations at the two PIV planes are compared with each other. As mentioned previously, the phase-averaged vorticity fields show that the cylinders do not impact the timing of the shear-layer rolling up. Thus, these cylinders do not modify the axisymmetry of the round jet as was demonstrated to be the case when the shape of the nozzle's exit was changed (Longmire *et al.*, 1992) or when tabs or vortex generators were installed at the jet's exit (Reeder & Samimy, 1996). However, the circulation magnitude at the two perpendicular planes do differ from one another in most cases with the cylinder. This observation conveys that the cylinders do change the axisymmetry of the jet, albeit in a subtle manner.

CONCLUDING REMARKS

In this paper the dynamics of a round jet subject to acoustic forcing were studied, in the presence of a circular cylinder located upstream of the jet exit. Cylinders of different diameters were installed at various upstream locations. Acoustic excitation was used to condition the jet flow field at a particular frequency. Phase-locked, high spatial-resolution planar PIV was employed to obtain quantitative velocity data in the jet's near field, especially in the developing shear layer. The PIV measurements were acquired at two perpendicular planes to discern the impact of the cylinders better.

The cylinders do not impact the mean flow field significantly. However, they diminish the strength of the vortical flow structures within the shear layer. This manifests as a reduction in the circulation within the vortical structure and leads to a decrease in the strength of the fluctuations within the flow field. The diminishing effects on various flow quantities was found to be proportional to the ratio x_C/d_C which indicates that the vortex shedding in the cylinder's wake interferes with the shear layer development and thus, the dynamics within the jet. Furthermore, while the cylinders are not seen to modify the timing of the shear layer rolling up (which is still dominated by the imparted acoustic excitation), the circulation magnitude at the two measured planes shows a difference which conveys that the axisymmetry of the round jet might be broken resulting in a more three-dimensional flow field, albeit in a subtle manner.

The observations made here may suggest that the cylinder modifies the inlet boundary condition of the jet. Thereby, it manipulates the strength of the Kelvin-Helmholtz instability mechanism prevalent in the near-field of the jet. The subtle increase in the flow's three dimensionality may also imply the cylinder impacting the secondary instabilities in the shear layer. These aspects will be investigated further in future works. A thorough parametric study is also necessary to better understand the trends observed here and to inspect if there is any fixed scaling involved. Finally, while the effects of the upstream cylinder on the jet flow are summarised here, the mechanisms that lead to these effects are not clear yet. Better insight into the mechanisms at play is of paramount importance and will be the focus of future research efforts.

ACKNOWLEDGEMENT

The authors gratefully acknowledge financial support from the European Research Council (ERC): Grant agreement 677931 TAIAC.

REFERENCES

Adrian, R.J., Christensen, K.T. & Liu, Z.-C. 2000 Analysis and interpretation of instantaneous turbulent velocity fields. *Experiments in fluids* **29** (3), 275–290.

Æsøy, E., Aguilar, J.G., Bothien, M.R., Worth, N.A. & Dawson, J.R. 2021*a* Acoustic-convective interference in transfer functions of methane/hydrogen and pure hydrogen flames. *Journal of Engineering for Gas Turbines and Power* **143** (12).

Æsøy, E., Aguilar, J.G., Worth, N.A. & Dawson, J.R. 2021*b* The response of an axisymmetric jet placed at various positions in a standing wave. *Journal of Fluid Mechanics* **917**.

Aydemir, E., Worth, N.A. & Dawson, J.R. 2012 The formation of vortex rings in a strongly forced round jet. *Experiments in fluids* **52** (3), 729–742.

Crow, S.C. & Champagne, F.H. 1971 Orderly structure in jet turbulence. *Journal of Fluid Mechanics* **48** (3), 547–591.

Gharib, M., Rambod, E. & Shariff, K. 1998 A universal time scale for vortex ring formation. *Journal of Fluid Mechanics* **360**, 121–140.

Ho, C.M. & Huerre, P. 1984 Perturbed free shear layers. *Annual Review of Fluid Mechanics* **16** (1), 365–422.

Longmire, E.K. & Duong, L.H. 1996 Bifurcating jets generated with stepped and sawtooth nozzles. *Physics of Fluids* **8** (4), 978–992.

Longmire, E.K., Eaton, J.K. & Elkins, C.J. 1992 Control of jet structure by crown-shaped nozzles. *AIAA journal* **30** (2), 505–512.

Reeder, M.F. & Samimy, M. 1996 The evolution of a jet with vortex-generating tabs: real-time visualization and quantitative measurements. *Journal of Fluid mechanics* **311**, 73–118.

Reynolds, W.C., Parekh, D.E., Juvet, P.J.D. & Lee, M.J.D. 2003 Bifurcating and blooming jets. *Annual Review of Fluid Mechanics* **35** (1), 295–315.

Seybert, A.F. & Ross, D.F. 1977 Experimental determination of acoustic properties using a two-microphone random-excitation technique. *Journal of the Acoustical Society of America* **61** (5), 1362–1370.

Worth, N.A., Mistry, D., Berk, T. & Dawson, J.R. 2020 Vortex dynamics of a jet at the pressure node in a standing wave. *Journal of Fluid Mechanics* **882**.